Available online at www.sciencedirect.com

SciVerse ScienceDirect

Ceramics International 38 (2012) 4645–4651

CERAMICS
INTERNATIONAL

www.elsevier.com/locate/ceramint

Synthesis of supported fibrous nanoceramics via electrospinning

K. Starbova [a], D. Petrov [b,*], N. Starbov [a], V. Lovchinov [a]

[a] *Institute of Solid State Physics, Bulgarian Academy of Sciences, 72, Tzarigradsko Chaussee, 1784 Sofia, Bulgaria*
[b] *University of Food Technologies, Department of Inorganic and Physical Chemistry, 26, Maritsa Blvd., Plovdiv 4002, Bulgaria*

Received 20 January 2012; accepted 8 February 2012
Available online 21 February 2012

Abstract

Stable homogeneous aqueous spinning solutions have been experimented under electro-hydrodynamic conditions in order to synthesize fibrous ZnO, TiO_2 and Al_2O_3. A favourable combination of optimal solution, electrospinning, thermal post-processing and calcination parameters have provided the preparation of dense webs of fibres with a mean diameter in the nanosized range. The samples have been characterized by electron imaging under SEM and HRTEM. Conventional WAXRD and SAED have been applied to determine the phase composition. Simple mechanical and gas flow tests give a first evidence for building of fibre-to-fibre and web-to-substrate cohesive forces. The fibre immobilization has been found very important for the development of various functional ceramic materials.

Keywords: A. Precursors: organic; B. Fibres; B. Electron microscopy; B. X-ray methods; D. Transition metal oxides

1. Introduction

The electrospinning could be regarded as a contemporary top-down approach for synthesis of meso-, micro- and nanosized fibrous materials with high length-to-diameter ratio and porosity, high specific surface area and a controllable mean grain size [1–3]. The renewed interest to that relatively inexpensive, simple and exceptionally versatile technique could be primarily attributed to the synthesis of a broad set of low dimensional continuous, nanostructured fibres and possibilities for their alignment and spooling, chemical functionalization, etc. [4–6]. The revival and refinement of the electrospinning technique has remarkably expanded the wealth of engineered fibrous materials prepared from large number of organic and inorganic precursor solutions. Thus, an important class of fibre nanomaterials appeared encompassing simple, binary and ternary oxide ceramics [7–12]. The reasonable expectations for significant changes in the values of basic-structure related properties, such as electrical conductivity, chemical and photochemical activity and mechanical stability have been already supported by experimental evidences [13,14]. Moreover, since the oxide ceramics are also biocompatible, novel electrospun fibrous materials for medical application have been successfully synthesized [15].

Nowadays, there is a continuous trend for synthesis of fibrous ceramics via electrospinning with novel chemical and phase composition and amazing morphologies [9]. It seems, therefore, that the choice of proper assisting polymers, inorganic precursors, corresponding solvents and electrospinning conditions, is a relatively easy task. However, in order to get closer to the synthesis of real applied products, the purely academic studies should be reoriented so as to fulfil also the corresponding practical requirements. An important intermediate step in that direction should be the immobilization of the obtained non-woven mats over appropriate substrates. In our opinion, the building-up of both strong fibre-to-fibre and fibre web-to-substrate adhesive forces is one of the basic requirements for the development of applied products with supported functional fibrous ceramic media. As known, the latter are synthesized predominantly subjecting to electrospinning polymer/sol–gel blend spinning solutions (see for example [2,4,8]). From our experience it follows that, as a rule, in those cases the resulting as spun, polymer free and calcinated mats are three-dimensional with insufficient fibre-to-fibre bonding, if any, lacking of any adhesion to the substrate. Due to the relative high vapour pressure of the liquid metal-organic precursors and organic solvents used, fibres with specific concentration and distribution of dangling bonds dry completely during the time

---

* Corresponding author. Tel.: +359 32603621; fax: +359 32644102.
E-mail addresses: ellhnas1@abv.bg, petrov_d_n@abv.bg (D. Petrov).

0272-8842/$36.00 © 2012 Elsevier Ltd and Techna Group S.r.l. All rights reserved.
doi:10.1016/j.ceramint.2012.02.046

of flight between the spinneret and the collector. Thus, a self-supported non-woven mat with very low fracture toughness is accumulated on the latter. Since under the same conditions the water vapour pressure is relatively lower as compared to that of the most organic solvents used, we have tried to find the magic key in preparing blend aqueous polymer/ceramic precursor spinning solutions. The observed initial pseudo-adhesion of polymer fibres to the collector seemed to us a substantial prerequisite for obtaining supported fibrous ceramics via electrospinning. We have chosen the high molecular polyethylene oxide (PEO) as a partner polymer since, except for the proven merit to be electrospun, it assists the spinnability of blend solutions, adheres to different substrate surfaces and could be easily removed from hybrid fibres via thermal degradation [16–19]. Moreover, PEO is biocompatible and therefore suitable for devices contacting with living organisms [20].

Alternatively, we have tried to replace the alkoxide ceramic precursors solutions prepared via conventional sol–gel procedure by aqueous solutions of metal-organic salts. Thus, in the present study an experimental strategy has been applied for simple and reproducible preparation of blend polymer/inorganic precursor spinning solutions. The latter have been further subjected to electrospinning in order to study the opportunities for synthesis and immobilization of non-woven mats of ZnO, TiO_2 and Al_2O_3 on solid state substrates. These are the main goals of the present work.

2. Experimental

2.1. Materials

As noticed above, water soluble polymer and organometallic salts have been chosen for the preparation of the spinning solution. All chemicals have been used without further purification. Distilled deionized water (conductivity < 0.5 μS/cm) has been used from considerations of both purity and electrical conductivity.

2.1.1. Polymers

PEO with an average relative molar mass $M_r = 800{,}000$ (800 kDa) and 1,000,000 (1 MDa) as determined in distilled water at 30 °C, using an Ubbelohde viscometer, by the equation: $[\eta] = 1.25 \times 10^{-4}$ $Mr^{0.78}$ has been used as high molecular polymer [16].

The starting polymer solutions have been prepared using PEO with different mass concentration (%) depending on the ceramic precursor solutions. 8.0% and 6.0% aqueous PEO ($M_r = 800$ kDa) solutions have been mixed with the precursors solutions of Zn or Al correspondingly. For preparing of Ti containing blend spinning solution 3.0% aqueous solution of PEO ($M_r = 1.0$ MDa) has been used.

2.1.2. Ceramic precursors

Our preliminary studies on the preparation of other aqueous blend spinning solutions unambiguously showed that at hydrolysis in the low pH range the high molecular PEO depolymerises thus loosing its ability to be electrospun and, therefore, to assist the electrospinning [15]. For that reason, we have selected among the variety of ceramic precursor ingredients water soluble salts of the CH_3COOH, $Zn(CH_3COO)_2$ – ZnAc, $Al(CH_3COO)_3$ – AlAc and $Ti(CH_3OOH)_4$ – TiAc. The pH value of their solutions varied in the range 5.0–6.0, hence, the depolymerization degree of PEO is low. We have used saturated aqueous solution of ZnAc dissolving $Zn(CH_3COO)_2{\cdot}2H_2O$ (≥98%, Sigma Aldrich) in deionized water under magnetic stirring.

Further, we have applied a rapid method for modification of commercially available basic aluminium acetate, $Al(OH)(CH_3CO_2)_2$ to the $Al(CH_3COO)_3$, characterized by a higher aqueous solubility. Tartaric acid ($C_4H_6O_6$) 1.5 g has been dissolved in 30 cm^3 deionized water. Then, to that aqueous solution 1.62 g $Al(OH)(CH_3COO)_2$ (Purum, Sigma Aldrich) with 0.6 cm^3 glacial, 100% CH_3COOH (≥99.7% Sigma Aldrich) have been added. The obtained suspension has been further boiled for 2–2.5 h in closed vessel until $Al(OH)(CH_3COO)_2$ is dissolved. Thus, we have obtained the solution of AlAc containing 0.75% Al [21].

Since the titanium acetate – TiAc, has not been an object of production interest of the leading chemical companies, we have found an experimental approach for its preparation via modification of $Ti(OR)_4$ in the presence of CH_3COOH [22]. It has been observed that a substitution of radicals OR and direct acetates bonding to titanium as revealed on the IR spectra, provide both chelating and bridging acetates. The initial part of the experimental procedure has been carried out using $Ti(OC_3H_7)_4$ as starting alcoxide. We have added dropwise 4 cm^3 glacial CH_3COOH (≥99.7% Sigma Aldrich) to 5 cm^3 $Ti(OC_3H_7)_4$ (97% Sigma Aldrich) under magnetic stirring for 10 min. An exothermic reaction took place leading to clear and stable $Ti(C_3OOH)_4$ – TiAc solution. The latter, after cooling, represented our titanium precursor solution containing 16% Ti.

2.1.3. Preparation of blend solutions

The blend spinning solutions have been prepared via dropwise addition of saturated aqueous solution of ZnAc (a) and laboratory prepared solutions of AlAc (b) and TiAc (c) to the corresponding, gently stirred PEO solution. The weight ratio of the blend spinning solutions used displaying optimal viscous–elastic properties under electrospinning conditions are, respectively, as follows: 8.0% PEO (800 kDa)/ZnAc = 2:1, 5.0% PEO (800 kDa)/AlAc = 1:1, 3.0% PEO (1.0 MDa)/TiAc = 5:1.

2.2. Electrospinning procedure

The solutions have been passed through a syringe with a stainless steel needle at the tip. The needle has been electrified using a high-voltage DC supply with an applied high voltage. The solution has been pumped continuously using a syringe pump at an approx. flow rates of 0.1 cm^3/h, 0.4 cm^3/h and 0.5 cm^3/h for TiAc, AlAc or ZnAc, respectively.

A grounded collector of thick aluminium foil served as a counter electrode. The applied field strength – AFS, between the capillary tip and counter electrode was of the order of

1.0 kV/cm. Pieces of soda lime glass, sheet stainless steel (SAE 202 grade) and aluminium foil arranged over the collector, served as substrates. White coloured as spun hybrid fibres have been collected well adhered to these substrates.

2.3. Thermal processing

In order to obtain PEO free ceramic fibres a part of the hybrid non-woven mats from all samples have been further placed in a quartz tubular furnace and thermally modified via specially developed two-step calcination under non-isothermal conditions at a mean heating rate of 1.0 °C/min. The samples have been held at 120 °C and at 360 °C related to water and PEO removal correspondingly. The presence of low-pressure oil-free compressed air, has provided conditions for the efficient removal of the emanating gases from the heated space and controlled PEO pyrolysis [23,24].

The thermally processed PEO free non-woven mats are also white coloured like the as spun ones. Except for an efficient PEO removal this thermal processing favours also the transition of amorphous ZnO and TiO_2 fibres to crystalline ones. These samples have been held at 360 °C for 2 h. The PEO free mats of Al- and Ti-based samples have been subjected further to calcination in the presence of low-pressure oil-free compressed air 2 h at 500 °C and 550 °C at 5 h maintaining a constant heating rate of the order of 1.0 °C/min.

In addition to PEO removal and crystallization, the thermal processing steps described above have displayed additional apparent effects. These are manifested in a withstanding of the supported mats to high air pressures – at least 2.0 bar, as well as impossibility to be detached from the substrates by means of razor blade. Therefore, the applied thermal procedure favours fibres-to-fibres and mats-to-substrate binding most probably by strong chemical bonding at their contact surfaces.

2.4. Sample characterization

Scanning electron microscope Philips 515 has been used for studying the morphology of as spun, PEO free and thermally processed samples. The samples have been previously coated under high vacuum conditions with consecutive carbon and gold layers. The phase compositions of the thermally processed mats have been verified by conventional wide angle X-ray diffraction – WAXRD, by means of APD – 15 Philips X-ray diffractometer. For Ti-based samples the data have been complemented by electron optical imaging via selected area electron diffraction – SAED, performed under high resolution transmission electron microscope – HRTEM, JEOL 2100. Sample preparation for HRTEM observations have consisted of deliberate glass substrate crashing, a careful detachment of a small part of fibre web retained at the crashed periphery and fixing on electron microscope grids by means of conductive silver paste. It is important to note here that the TiO_2 fibrous web detached from the substrate and used for HRTEM imaging and electron diffraction, displayed some degree of plasticity. For that reason, it has been easy to be handled during the preparation stage. In order to determine the fibre diameter distribution, statistical measurements have been performed using Image J – U.S. NIH computer software. A minimum of 20 fibre diameters has been measured for each sample.

3. Results and discussion

3.1. Micromorphology

Several aqueous blend solutions with different PEO/acetate mass ratios and corresponding PEO controls of 5.0% (800 kDa) and 3.0% (1 MDa) have been tested for fibre forming ability under electrospinning conditions described in the experimental part. It has been established that similarly to the solutions of the polymers themselves, the mixed solutions are also capable to be electrospun in fibre-like form. Optimal combinations of spinning solutions and electrospinning parameters have been chosen as noted in the experimental part on the basis of the observations under the scanning electron microscope.

Fig. 1 presents low and high magnification scanning electron micrographs of PEO free calcinated ZnO (a), TiO_2 (b) and Al_2O_3 (c) fibres obtained from optimal blend spinning solutions at AFS 1.0 kV/cm. The PEO (800 kDa) fibres electrospun from 5.0% aqueous solution are also given for comparison (d). It is clearly seen the synthesis of defect free ceramic fibres, preserving the pliability PEO samples (d). For that reason, fibre-to-fibre contacts are preserved, thus inducing strong cohesive forces. Except for minor differences in the mean fibre diameter, the micrographs in Fig. 1(a–c) are also typical for the as spun mats of the hybrid fibres. On this basis it could be concluded that the final fibre morphology is determined by that of the assisting high molar mass polymer, the pliability of latter playing a decisive role on the fibre immobilization.

The scanning electron micrographs in Fig. 2 demonstrate an opportunity to build up ZnO fibrous scaffold performing the thermal processing at a threefold increased mean heating rate – 3.0 °C/min, compared to the optimal one of 1.0 °C/min (Fig. 1a). Obviously, the higher heating rate favours the occurrence of initial stages of melting resulting in bunched together fibres situated each over the other. It is then reasonable to conclude that this local process takes place within the polymer ingredient of the hybrid fibres, since the melting point of ZnO is far from that temperature. In our opinion, the synthesis of fibrous scaffold via electrospinning has to be also of practical interest because of the reasonably high cohesion degree of fibre-to-fibre as well as web-to-substrate adhesion.

The results from the statistical measurements performed for all samples evidence a fibre diameter distribution in the nanosized range, the mean fibre values being in the range 400–450 nm, 180–220 nm and 100–120 nm for ZnO, TiO_2 or Al_2O_3 samples, respectively. Moreover, in spite of the differences in the polymer/inorganic precursor mass ratio of the optimal spinning solutions used the mean diameter of the thermally nonprocessed as spun hybrid fibres is only approx. 10% higher that of the PEO free ceramic fibres. It seems, therefore, that the

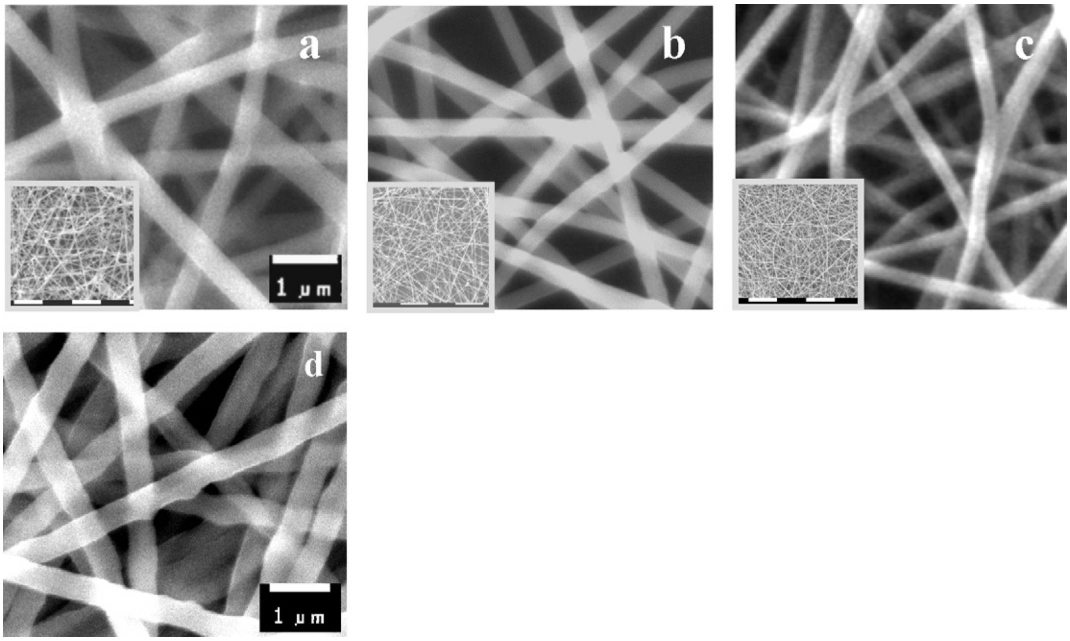

Fig. 1. Scanning electron micrographs of electrospun PEO free, calcinated ZnO (a), TiO_2 (b) and Al_2O_3 (c) fibres; mean heating rate of 1.0 °C/min; (d) electrospun PEO (800 K); AFS 1.0 kV/cm.

latter should be characterized by a considerable degree of porosity. This statement is supported to a certain extent by the high resolution transmission electron micrograph of PEO free calcinated TiO_2 fibres in Fig. 3.

As could be seen from the micrograph the fibres are built up of nanosized grains separated by a low density network. Besides, the enlarged area additionally reveals a specific grain arrangement. It should be concluded that synthesis of fibrous samples under electrospinning conditions is simultaneously accompanied by twisting along the fibre axis. Obviously, fibre self-decoration takes place, the grains playing role of decorating "agent". From the most general point of view the low mean heating rate used favours the occurrence of this visualization process.

3.2. Phase composition

3.2.1. ZnO

Fig. 4 shows WAXRD spectrum of PEO free non-woven mat from ZnO fibres obtained from blend aqueous solution of 8.0% POE (800 kDa and saturated aqueous ZnAc solution in 2:1 weight ratio at AFS 1.0 kV/cm. The electrospinning fibres deposition has been followed by two step post processing of the non-woven mat in non-isothermal regime performed at a mean heating rate of 1.0 °C/min. It is seen from the X-ray diffractogram presented an intense peak resolved at $2\theta = 34.32^\circ$, and weak satellite peaks at $2\theta = 31.8^\circ$ and 36.3°, all typical for wurtzite crystal structure. In spite of the random fibre distribution on the substrate the ZnO sample is

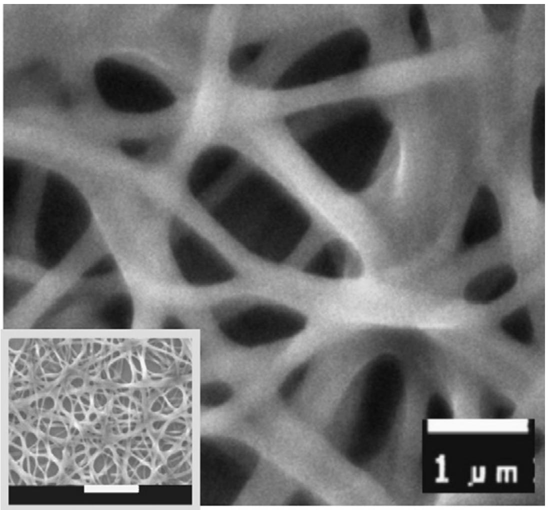

Fig. 2. Scanning electron micrograph of electrospun PEO free ZnO fibres.

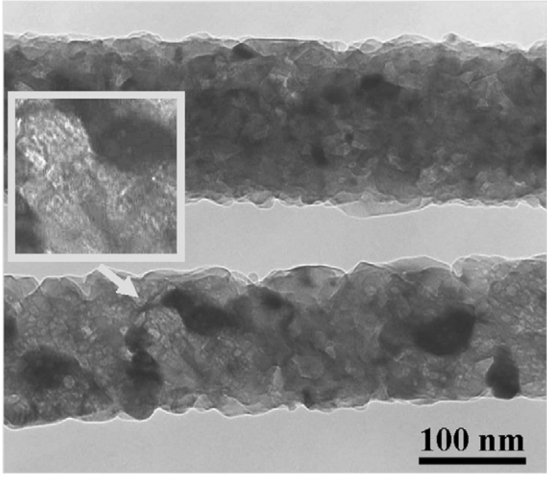

Fig. 3. High resolution transmission electron micrograph of PEO free calcinated (2 h at 500 °C) TiO_2 fibres; mean heating rate 1.0 °C/min; AFS 1.0 kV/cm.

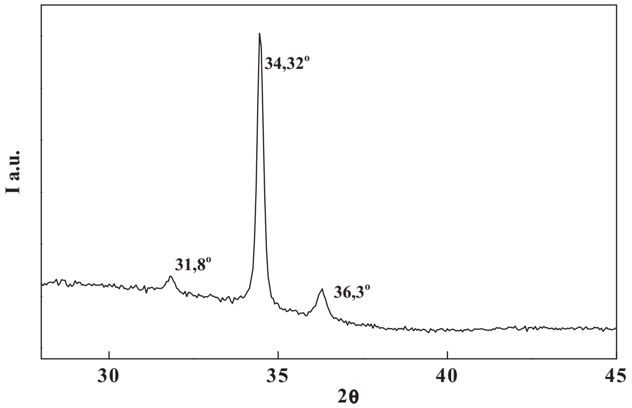

Fig. 4. WAXRD spectrum of PEO free, calcinated (360 °C, 2 h) ZnO fibres; mean heating rate 1.0 °C/min; AFS 1.0 kV/cm.

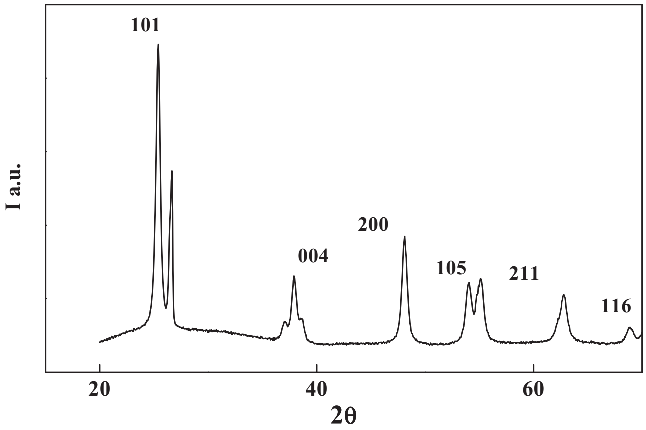

Fig. 6. WAXRD spectrum of PEO free, calcinated (500 °C, 2 h) TiO_2 fibres; mean heating rate 1.0 °C/min; AFS 1.0 kV/cm.

textured, the fibre axes coinciding most likely with [0 0 2] crystallographic direction.

Any assumption for the relationship between the preferred orientation of ZnO crystalline grains and the occurrence of fibre twisting during the time of flight between the spinneret and the collector would be highly speculative. Future HRTEM electron imaging and analysis will help in obtaining more detailed information.

3.2.2. TiO_2

Fig. 5 presents WAXRD spectrum of PEO free titanium based fibre web, calcinated for 2 h at 360 °C. Obviously, the applied thermal processing conditions favour fibre crystallization to anatase titania polymorph ($2\theta = 25.6°$). Similarly to the WAXRD pattern of ZnO (Fig. 4), fibre texturing is also observed, in that case along [1 0 1] crystallographic axis. Additional crystalline peaks appear subjecting anatase fibrous samples to further calcinations at higher temperature. This is demonstrated in Fig. 6 by the recorded WAXRD of PEO free Ti–O fibres calcinated 2 h at 500 °C. Detailed analysis of X-ray diffraction data of samples reveals anatase polymorph of titania, as well as a strong peak at $2\theta = 26.66°$ ($d = 3.34$ Å) that could be attributed to Ti–O with lower oxygen content as Ti_8O_{15} [25].

The lower intensity peaks correspond to the brookite TiO_2 polymorph modification [26]. On this basis it could be assumed that a partial chemical reduction takes place provided the calcination of Ti-based fibres has been performed at 500 °C, resulting in the evolution of oxygen deficient Ti–O crystalline phase. This assumption is supported by analytical data on the presence of intermediate or end products of PEO pyrolisis as acetaldehyde, formaldehyde and CO with pronounced reduction properties [16].

In the present study, semi-quantitative evaluation of the mean crystallite size of particles constituting the fibres of calcinated mats has been performed applying Scherrer's formula to the most intense diffraction peaks. Nanosized crystallites with mean crystallite size of 19 nm, 16 nm, and 31 nm for (1 0 1) anatase, (2 1 0) brookite and those of oxygen deficient titanium oxide have been correspondingly estimated.

Additional analytical studies have been performed under TEM since the highest intensity peaks of anatase (1 0 1) and brookite (1 2 0) are known to overlap. Fig. 7 presents SAED pattern of calcinated TiO_2 fibres (a) and HRTEM image (b) of a single crystalline grain (b). As could be expected, Fig. 7 (a) displays SAED pattern that is typical for a polycrystalline sample. The results from SAED diffraction analysis performed have revealed crystalline phases of both anatase and brookite

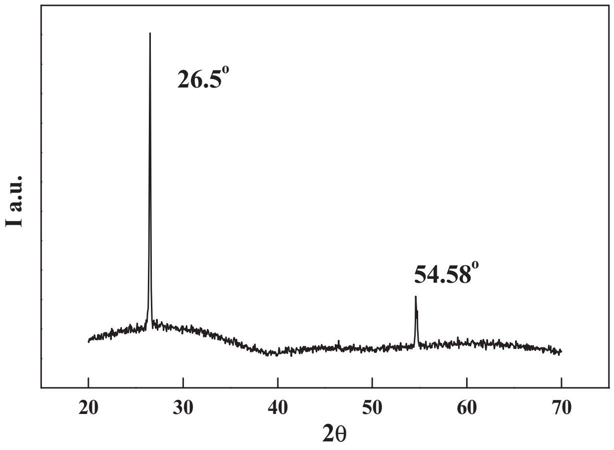

Fig. 5. WAXRD spectrum of PEO free, calcinated (360 °C, 2 h) TiO_2 fibres; mean heating rate 1.0 °C/min; AFS 1.0 kV/cm.

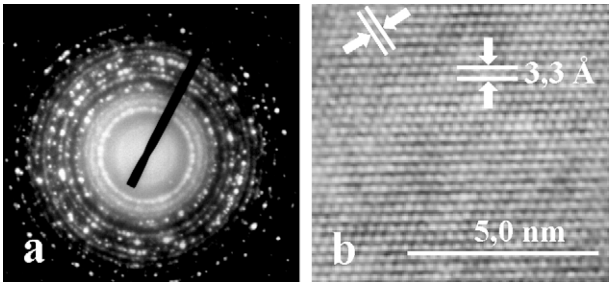

Fig. 7. SAED (a) and two dimensional HRTEM bright field image (b) of a TiO_2 grain in calcinated fibres; mean heating rate 1.0 °C/min; AFS 1.0 kV/cm.

TiO_2 polymorph while the high resolution bright field image of single grain corresponds to anatase (1 0 1) crystalline phase.

In summary, the results obtained clearly demonstrate that depending on the thermal postprocessing conditions immobilized defect-free electrospun fibrous TiO_2 samples could be synthesized with different phase composition.

3.2.3. Al_2O_3

A great variety of low and high temperature alumina crystalline polymorphs can be synthesized using aluminium complex precursors via transition sequences as dependent on the thermal processing conditions applied [27]. The problem for preparation of supported nanostructured alumina with desired crystalline structure via thermal crystallization faces also requirements towards the substrates used for their immobilization. Provided the substrate thermal stability at the corresponding temperature has been achieved, optimal thermal expansion coefficient and low degree of thermal diffusion of substrate ingredients within the samples are ensured, the initial morphology of hybrid fibres should be preserved. Because of the specific spinel structure some low temperature alumina crystalline polymorphs have found a broad application in supported materials in catalysis [28].

For that reason, in the present study 202 grade stainless steel sheets have been used as substrates for deposition of electrospun fibres obtained from solutions containing aluminium precursor. As mentioned above, the hybrid non-woven mats have been subjected to consecutive two step procedure for water – at 120 °C, and at 360 °C – for POE removal, followed by calcination for 5 h at 550 °C. Fig. 8 presents XRD of samples obtained using stainless steel substrate. Aside from the high intensity stainless steel peaks, low intensity peaks evidence initial crystallization stages of the fibres. They could be attributed to cubic γ-Al_2O_3 at 2θ range below 33° [29]. Future experiments on improving the calcination conditions, complementing X-ray by electron diffraction and HRTEM imaging will help in obtaining electrospun PEO free fibres of desired low temperature modification of Al_2O_3. The perfect fibre web morphology (Fig. 1c) and its stability during the thermal processing at 500 °C are prerequisites for the success of further experiments.

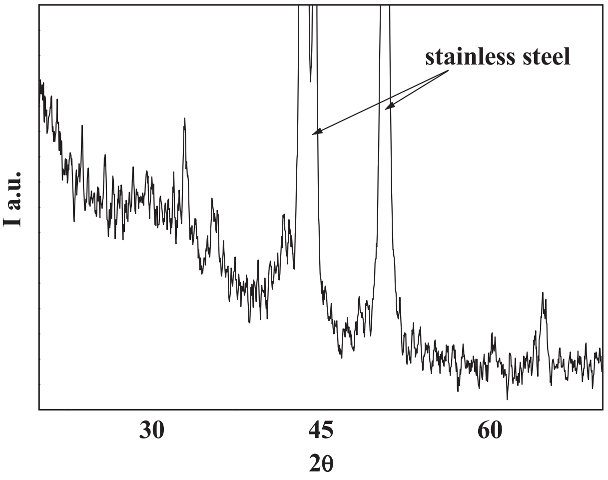

Fig. 8. WAXRD spectrum of PEO free, calcinated (5 h at 550 °C) non-woven mat from Al/O fibres; mean heating rate 1.0 C/min; AFS 1.0 kV/cm.

4. Conclusion

The present experimental study emphasizes the importance of fibre immobilization for the development of fibrous supported functional materials via electrospinning. An experimental opportunity is proposed for synthesis and immobilization of electrospun ZnO, TiO_2 and Al_2O_3 fibres. The use of both water soluble high molar mass PEO as assisting polymer and aqueous free solutions of corresponding metal acetates, are considered to be the key elements for preparing the spinning solutions and thus for fibre synthesis itself. In addition, it is shown that the choice of optimal thermal postprocessing conditions provides preservation of fibre web morphology in the sequence hybrid-PEO free-calcinated fibres. It seems that the inherent pliability of the electrospun PEO fibres is of a crucial importance for the successive occurrence in all stages of the synthesis. Similarly to the control PEO fibre morphology, dense webs consisting in one-dimensional defect free fibres bonded at their contact surfaces, are demonstrated by secondary electron imaging. Thus, the results obtained reveal more efficient viscous–elastic behaviour of the high molar mass PEO under electro-hydrodynamic conditions compared to that of PVA used for synthesis of ZnO fibres by similar processing route [30–33]. The results from simple mechanical and gas flow pressure tests performed give evidence for fibre-to-fibre bonding as well as the building of adhesion forces between the fibre web and the substrate. Further experiments on the application of the synthesis route described for designing of other supported fibrous functional materials are in progress.

Acknowledgements

This paper is completed with the financial support of Bulgarian National Fund ‘‘Scientific Research’’ under contract 04-II/2004.

The authors are greatly acknowledged to Prof. B. Angelov – Dept. of Inorganic and Physical Chemistry, University of Food Technologies – Plovdiv, for some grammar recommendations and corrections of the final manuscript.

References

[1] A. Formhals, US Patent 1,975,504, 1934.
[2] D.H. Reneker, I. Chun, Nanometer diameter fibers of polymer, produced by electrospinning, Nanotechnology 7 (1996) 216–223.
[3] D. Li, Y. Xia, Electrospinning of nanofibers: reinventing the wheel, Adv. Mater. 16 (2004) 1151–1170.
[4] W. Sigmund, J. Yuh, H. Park, V. Maneeratana, G. Pyrgiotakis, A. Daga, J. Taylor, J. Nino, Processing and structure relationships in electrospinning of ceramic fiber Systems, J. Am. Ceram. Soc. 89 (2006) 395–407.
[5] E. Formo, P.H.C. Camargo, B. Lim, M.J. Jiang, Y.N. Xia, Functionalization of ZrO_2 nanofibers with Pt nanostructures: the effect of surface roughness on nucleation mechanic and morphology control, Chem. Phys. Lett. 476 (2009) 56–61.

[6] E. Formo, E. Lee, D. Campbell, Y.N. Xia, Functionalization of electrospun TiO_2 nanofibers with Pt nanoparticles and nanowires for catalytic applications, Nano Lett. 8 (2008) 668–672.

[7] G. Larsen, R.V. Ortiz, K. Minchow, A. Barrero, I.G. Loscertales, A method for making inorganic and hybrid (organic/inorganic) fibers and vesicles in the micrometer and sub-micrometer range via sol–gel chemistry and electrically forced liquid jets, J. Am. Chem. Soc. 125 (2003) 1154–1155.

[8] Y. Wu, L.L. Hench, J. Du, K.L. Choy, J.K. Guo, Preparation of hydroxyapatite fibers by electrospinning technique, J. Am. Ceram. Soc. 87 (2004) 1988–1991.

[9] Y. Dai, W. Liu, E. Formo, Y. Sun, Y. Xia, Ceramic nanofibers fabricated by electrospinning and their applications in catalysis, environmental science, and energy technology, Polym. Adv. Technol. 22 (2011) 326–338.

[10] A.F. Lotus, Y.C. Kang, J.I. Walker, R.D. Ramsier, G.G. Chase, Effect of aluminum oxide doping on the structural, electrical, and optical properties of zinc oxide (AOZO) nanofibers synthesized by electrospinning, Mater. Sci. Eng. B 166 (2010) 61–66.

[11] Y. Gu, D. Chen, X. Jiao, Synthesis and electrochemical properties of nanostructured $LiCoO_2$ fibers as cathode materials for lithium-ion batteries, J. Phys. Chem. B 109 (2005) 17901–17906.

[12] Y. Gu, D. Chen, X. Jiao, F. Liu, $LiCoO_2$–MgO coaxial fibers: co-electrospun fabrication, characterization and electrochemical properties, J. Mater. Chem. 17 (2007) 1769–1776.

[13] R. Zhu, C.Y. Jiang, X.Z. Liu, B. Liu, A. Kumar, S. Ramakrishna, Improved adhesion of interconnected TiO_2 nanofiber network on conductive substrate and its application in polymer photovoltaic devices, Appl. Phys. Lett. 93 (2008) 1529–1532.

[14] M.Y. Song, D.K. Kim, K.J. Ihn, S.M. Jo, D.Y. Kim, Electrospun TiO_2 electrodes for dye-sensitized solar cells, Nanotechnology 15 (2004) 1861–1865.

[15] K. Starbova, E. Krumov, D. Karashanova, N. Starbov, Polyoxyethylene assisted electrospinning of nanofibers from calcium phosphate sol solution, J. Optoelectron. Adv. Mater. 11 (2009) 1319–1322.

[16] J. Brandrup, E.H. Immergut, Polymer Handbook, third ed., John Wiley & Sons, New York, 1989.

[17] H. Fong, I. Chun, D.H. Reneker, Beaded nanofibers formed during electrospinning, Polymer 40 (1999) 4585–4592.

[18] J.M. Deitzel, J. Kleinmeyer, J.K. Hirvonen, N.C.B. Tan, Controlled deposition of poly(ethylene oxide) fibers, Polymer 42 (2001) 8163–8170.

[19] K. Starbova, M. Spasova, V. Yordanova, N. Starbov, I. Rashkov, Polyethylene oxide assisted synthesis of titania fibers via electrospinning, J. Optoelectron. Adv. Mater. – Rapid Commun. 1 (2007) 629–635.

[20] D.A. Herold, K. Keil, D.E. Burns, Oxidation of PEG by alcohol dehydrogenase, Biochem. Pharmacol. 38 (1989) 73–76.

[21] I. Yuko, M. Teruo, Y. Ryoko, S. Mashiko, Pharmaceutic and pharmacological evaluation of Burow's solution (aluminium acetate), J. Pharm. Soc. Jpn. 124 (2004) 833–840.

[22] S. Doeuff, M. Henry, C. Sanchez, J. Livage, Hydrolysis of titanium alkoxides: modification of the molecular precursor by acetic acid, J. Non-Cryst. Solids 89 (1987) 206–216.

[23] E. Neumann, H. Nadeau, Analysis of polyether and polyolefin polymers by gas chromatographic determination of the volatile products resulting from controlled pyrolysis, Anal. Chem. 35 (1963) 1454–1457.

[24] K. Starbova, E. Krumov, N. Starbov, M. Spasova, I. Rashkov, Zirconia–polyethylene oxide composite electrospun fibers for tissue engineering, in: E. Balabanova, I. Dragieva (Eds.), Nanoscience & Nanotechnology, vol. 6, Heron Press, Sofia, 2006, pp. 237–242.

[25] Powder Diffraction File, Fiche No. 18-1404.

[26] Powder Diffraction File, Fiche No. 29-1360.

[27] S. Cava, S.M. Tebcherani, I.A. Souza, S.A. Pianaro, C.A. Paskocimas, E. Longo, J.A. Varela, Structural characterization of phase transition of Al_2O_3 nanopowders obtained by polymeric precursor method, Mater. Chem. Phys. 103 (2007) 394–399.

[28] M. Trueba, S.P. Trasatti, γ-Alumina as a support for catalysts: a review of fundamental aspects, Eur. J. Inorg. Chem. 17 (2005) 3393–3403.

[29] Powder Diffraction File, Fiche No. 79 1557.

[30] X. Yang, C. Shao, H. Guan, X. Li, J. Gong, Preparation and characterization of ZnO nanofibres by using PVA/zinc acetate composite fiber as precursor, Inorg. Chem. Commun. 7 (2004) 176–178.

[31] H. Ren, Y. Ding, Y. Jiang, F. Xu, Z. Long, P. Zhang, Synthesis and properties of ZnO nanofibers prepared by electrospinning, J. Sol–Gel Sci. Technol. 52 (2009) 287–290.

[32] R. Siddheswara, R. Sankar, M.R. Babu, M. Rathnakumari, R. Jayavel, P. Murugakoothan, P. Sureshkumar, Preparation and characterization of ZnO nanofibers by electrospinning, Cryst. Res. Technol. 41 (2006) 446–449.

[33] N. Sankhaprom, P. Supaphol, V. Pavarajarn, Fibrous zinc oxide prepared by combined electrospinning and solvothermal techniques, Ceram. Int. 36 (2010) 357–363.